0026-895X/08/7302-305–313$20.00
MOLECULAR PHARMACOLOGY
Vol. 73, No. 2
41640/3294449
Mol Pharmacol 73:305–313, 2008
Printed in U.S.A.

Conformational Flexibility of Helix VI Is Essential for Substrate Permeation of the Human Apical Sodium-Dependent Bile Acid Transporter

Naissan Hussainzada, Akash Khandewal, and Peter W. Swaan

Department of Pharmaceutical Sciences, University of Maryland, Baltimore, Maryland

Received September 7, 2007; accepted October 29, 2007

ABSTRACT

The present study characterizes the methanethiosulfonate (MTS) inhibition profiles of 26 consecutive cysteine-substituted mutants comprising transmembrane (TM) helix 6 of the human apical Na^+-dependent bile acid transporter (SLC10A2). TM6 is linked exofacially to TM7 via extracellular loop 3. TM7 was identified previously as lining part of the substrate permeation path (*Mol Pharmacol* **70:**1565, 2006). Most TM6 cysteine replacements were well tolerated, except for five residues with either severely hampered (I229C, G249C) or abolished (P234C, G237C, G241C) activity. Disruption of protein synthesis or folding and stability may account for lack of activity for mutant P234C. Subsequent Pro234 amino acid replacement reveals its participation in both structural and functional aspects of the transport cycle. Application of polar MTS reagents (1 mM) significantly inhibited the activity of six mutants (V235C, S239C, F242C, R246C, A248C, and Y253C), for which rates of modification were almost fully reversed (except Y253C) upon inclusion of bile acid substrates or removal of Na^+ from the MTS preincubation medium. Activity assessments at equilibrative [Na^+] revealed numerous Na^+-sensitive residues, suggesting their proximity in or around Na^+ interaction sites. In silico modeling reveals the intimate and potentially cooperative orientation of MTS-accessible TM6 residues toward functionally important TM7 amino acids, substantiating TM6 participation during the transport cycle. We conclude a functional requirement for helical flexibility imparted by Pro234, Gly237, and Gly241, probably forming a "conformational switch" requisite for substrate turnover; meanwhile, MTS-accessible residues, which line a helical face spatially distinct from this switch, may participate during substrate permeation.

By coupling bile acid movement to the passive flow of Na^+ ions down their concentration gradient, the human apical Na^+-dependent bile acid transporter (ASBT; SLC10A2) concentrates bile acids within the cell interior. Viewed from a physiological perspective, ASBT effectively conserves the body's recirculating bile acid pool (Trauner and Boyer, 2003) in tandem with numerous active transporters expressed along the enterohepatic pathway. Because cholesterol provides the precursor molecule in FXR- and hepatic CYP7A-mediated bile acid synthesis (Chiang et al., 2001; Pauli-Magnus et al., 2005), ASBT also constitutes a key modulator of cholesterol homeostasis. Numerous studies have recently underscored the exploitive potential of ASBT in cholesterol-lowering therapies (Oelkers et al., 1997; Izzat et al., 2000; Huff et al., 2002; Li et al., 2004) and emphasizing the usefulness of this high-capacity, high-affinity transporter in prodrug targeting (Swaan et al., 1997; Balakrishnan and Polli, 2006; Geyer et al., 2006). Consequently, ASBT's unique pharmaceutical relevance coupled to the absence of a crystal structure has provided a strong impetus toward elucidation of its structure/function relationships.

Using cysteine mutagenesis and thiol modification (SCAM), our previous studies identified transmembrane (TM) domain 7 in forming part of the putative substrate permeation pathway (Hussainzada et al., 2006) with extracellular loop (EL) 3 containing Na^+ and bile acid interaction sites (Banerjee et al., 2008). We continue SCAM analysis along TM6 based on the following rationale: 1) our topology model published previously predicts that TM6 lies adjacent to and may interact with TM7 in forming a putative translocation pathway (Zhang et al., 2004); 2) EL3 amino acids link TM6 and TM7 membrane-

This work was supported, in part, by the National Institutes of Health under grant DK61425 (to P.W.S.).
Article, publication date, and citation information can be found at http://molpharm.aspetjournals.org.
doi:10.1124/mol.107.041640.

ABBREVIATIONS: ABST, apical sodium-dependent bile acid transporter; EL, extracellular loop; GDCA, glychodeoxycholic acid; MTS, methanethiosulfonate; MTSES, methanethiosulfonate ethylsulfonate; MTSET, [2-(trimethylammonium)ethyl]-methane-thiosulfonate bromide; MTSEA, (2-aminoethyl)-methanethiosulfonate; SCAM, substituted cysteine accessibility method; TM, transmembrane; TMD, transmembrane domain; TCA, taurocholic acid; sulfo-NHS-SS-biotin, sulfosuccinimidyl-2 (biotinamido)ethyl-1,3-dithiopropionate; MHBSS, modified Hanks' balanced salt solution; PBS, phosphate-buffered saline; WT, wild type.

spanning segments along the exofacial matrix; 3) the highly conserved nature of TM6 amino acids corroborate a potential role during transport; 4) presence of the charged, conserved Arg246, which could potentially participate in electrostatic interactions implicated previously during ligand binding (Banerjee et al., 2008); and finally, 5) the presence of two conserved proline residues (Pro234, Pro251), which have been shown in other membrane-bound carriers to provide cation binding sites and enable formation of conformational switches essential for substrate translocation (Deber et al., 1990; Sansom and Weinstein, 2000; Pajor and Randolph, 2005). As in our previous studies, the C270A mutant provides the scaffold for subsequent cysteine introduction as a result of its insensitivity to methanethiosulfonate (MTS) reagents. Therefore, the present study assesses MTS sensitivity of 26 consecutive cysteine mutants introduced along TM6 of hASBT, thereby providing novel insight into the molecular workings of the ASBT translocation cycle. We demonstrate a functional prerequisite for TM6 helical flexibility in global conformational changes to protein structure, leading to substrate turnover and the putative involvement of TM6 amino acids in lining portions of the permeation pathway.

Materials and Methods

Materials. [^{3}H]Taurocholic acid (0.2 Ci/mmol) was purchased from American Radiolabeled Chemicals, Inc., (St. Louis, MO); Taurocholic acid (TCA) and glycodeoxycholic acid (GDCA) were from Sigma (St. Louis, MO); and sulfosuccinimidyl-2 (biotinamido)ethyl-1,3-dithiopropionate (sulfo-NHS-SS-biotin) was from Pierce Chemical Co. (Rockford, IL). MTS reagents (2-aminoethyl)-methanethiosulfonate (MTSEA), [2-(trimethylammonium) ethyl] methanethiosulfonate (MTSET), and methanethiosulfonate ethylsulfonate (MTSES) were from Toronto Research Chemicals, Inc. (North York, ON, Canada). Cell culture media and supplies were obtained from Invitrogen (Carlsbad, CA). All other reagents and chemicals were of highest purity available commercially.

Cell Culture and Transient Transfections. COS-1 cells (American Type Culture Collection, Manassas, VA) were maintained in Dulbecco's modified Eagle's medium containing 10% fetal calf serum, 4.5 g/l glucose, 100 U/ml penicillin, and 100 μg/ml streptomycin (Invitrogen, Carlsbad, CA) at 37°C in a humidified atmosphere with 5% CO_2. Transient transfections were performed as described previously (Banerjee et al., 2005).

Site-Directed Mutagenesis. Site-directed mutations were incorporated into hASBT cDNA using the Quik Change site-directed mutagenesis kit from Stratagene (La Jolla, CA) and mutagenesis primers custom-synthesized and purchased from Sigma Genosys (St. Louis, MO). Plasmid purifications were performed using a kit from QIAGEN (Valencia, CA) and amino acid substitutions confirmed via DNA sequencing using an ABI 3700 DNA analyzer (Applied Biosystems, Foster City, CA) at the Plant-Microbe Genomics Facility of the Ohio State University (Columbus, OH).

Uptake Assay and Protein Membrane Expression. Initial rates of transport for each mutant were determined in transiently transfected COS-1 cells incubated in modified Hanks' balanced salt solution (MHBSS), pH 7.4, uptake buffer containing 5.0 μM [^{3}H]TCA at 37°C for 12 min. We have demonstrated that this uptake period ensures linear steady-state kinetics in conjunction with an optimal signal-to-noise ratio for subsequent [^{3}H]TCA analysis via liquid scintillation counting (Banerjee et al., 2005; Banerjee and Swaan, 2006; Hussainzada et al., 2006). Uptake was halted by a series of washes with ice-cold Dulbecco's phosphate-buffered saline, pH 7.4, containing 0.2% fatty acid free bovine serum albumin and 0.5 mM TCA. Cells were lysed in 350 μl of 1 N NaOH and subjected to liquid scintillation counting using an LS6500 liquid scintillation counter (Beckmann Coulter, Inc., Fullerton, CA) and total protein quantification using the Bradford protein assay (Bio-Rad Laboratories, Hercules, CA). Uptake activity was calculated as picomoles of [^{3}H]TCA internalized per minute per milligram of protein.

Protein expression was determined by washing transiently transfected COS-1 cells in PBS followed by lysis in 0.2 ml of lysis buffer B (25 mM Tris, pH 7.4, 300 mM NaCl, 1 mM $CaCl_2$, 1% Triton X-100, and 0.5% Sigma Protease Inhibitor Cocktail). Cell lysates were separated on a 12.5% SDS-polyacrylamide gel and transferred onto an Immuno-Blot polyvinylidene difluoride membrane (Bio-Rad Laboratories). Blots were probed with rabbit anti-ASBT primary antibody (1:1000) and visualized using goat anti-rabbit IgG/horseradish peroxidase-conjugated secondary antibody with chemiluminescent detection (ECL Plus Western Blot kit; GE Healthcare, Chalfont St. Giles, Buckinghamshire, UK). Levels of cell surface protein expression were measured via biotin labeling, wherein transiently transfected COS-1 cells were incubated with sulfo-NHS-SS-biotin for 30 min at room temperature (Wong et al., 1995; Mitchell et al., 2004). After several washes with PBS containing 0.1 mM $CaCl_2$ and 1.0 mM $MgCl_2$, cells were disrupted with lysis buffer B at 4°C for 20 min (Zhang et al., 2004), and biotinylated proteins were recovered overnight at 4°C using 100 μl of streptavidin agarose beads. Samples were eluted with SDS-polyacrylamide gel electrophoresis buffer and immunoblotting performed as described above. Blots were probed for positive and negative controls, the plasma membrane marker α-integrin (150 kDa) and the endoplasmic reticulum membrane protein calnexin (90 kDa), respectively, to assess the integrity of the biotinylation procedure (calnexin; data not shown). Relative hASBT membrane expression was standardized to integrin expression and quantified via densitometry as described previously (Hussainzada et al., 2006).

MTS Inhibition Studies. Sensitivity of mutants to charged, membrane-impermeant MTS reagents was determined by preincubation of transiently transfected COS-1 cells with either 1 mM MTSES, MTSET, or MTSEA for 10 min at room temperature. After MTS treatment, cells were washed twice in modified Hanks' balanced salt solution (Sigma) followed by [^{3}H]TCA uptake as described above. All MTS solutions were freshly prepared before each study because of the short aqueous half-life of these MTS reagents.

Cation and Substrate Protection Assays. To determine whether the presence or absence of Na^+ and/or bile acid substrates alters MTSEA labeling, transiently transfected COS-1 cells were washed twice in 1× PBS, pH 7.4, followed by coincubation with equal concentrations of MTSEA and GDCA (1 mM) prepared either in MHBSS or Na^+-free buffer (MHBSS except choline chloride entirely substitutes NaCl) for 10 min at room temperature. After preincubation treatments, cells were washed twice in either MHBSS, pH 7.4, or Na^+-free buffer and additionally equilibrated for 15 min at 37°C in these buffers followed by determination of [^{3}H]TCA uptake as described above. All control wells were treated identically. For each mutant transporter, uptake values were determined by taking a ratio of mutant uptake at each experimental condition versus mutant uptake for its respective unmodified control. We normalize mutant ratios to C270A by expressing mutant ratios for each condition as a percentage of C270A ratios calculated in the same manner.

Sodium Activation. Measurement of [^{3}H]TCA uptake at equilibrative extracellular Na^+ concentrations (12 mM; i.e., at equilibrium with cytosolic [Na^+]) was performed (uptake conducted as described above; choline chloride used as equimolar NaCl replacement) and expressed as a ratio of uptake at physiological (137 mM) Na^+ concentrations to determine overall sensitivity of each mutant to the presence/absence of Na^+. In theory, Na^+ ratios equal to 1 imply little measurable difference in transporter activity despite the scarcity of Na^+ ions, whereas fractions less than 1 indicate a greater necessity for physiological Na^+ concentrations for proper transport function of a mutant transporter.

Data Analysis. For each mutant, data are represented as mean ± S.D. of at least three different experiments with triplicate measurements. Data analysis was performed with Prism 4.0 (GraphPad Software, Inc., San Diego, CA) using analysis of variance with Dun-

nett's post hoc test. Data were considered statistically significant at $p \leq 0.05$.

Results

Cysteine Scan of TM6. Based on our topology model published previously (Zhang et al., 2004; Banerjee and Swaan, 2006), residues spanning Trp227 to Tyr253 are predicted to constitute TM6 of hASBT (Fig. 1A). High-sequence homology is observed among various evolutionarily diverse species for this protein region (Fig. 1B), which lies in intimate proximity to critical protein regions described previously (Hallén et al., 2000, 2002; Kramer et al., 2001; Hussainzada et al., 2006). Systematic cysteine substitutions were incorporated along TM6 followed by structural and functional analysis of mutant transporters.

Transport Activity and Membrane Expression of Cysteine Mutants. Because of its low background levels of bile acid transport (Hussainzada et al., 2006), the COS-1 cell line was used to transiently express all TM6 mutant transporters. Surface biotin labeling of membrane-expressed proteins was accomplished using the membrane-impermeant sulfo-NHS-SS-biotin and quantified via densitometry of protein bands (Fig. 2B). ASBT bands for each sample were standardized to an internal control (α-integrin) and expressed as a percentage of C270A intensity (Fig. 2C). Initial transport activities (Fig. 2A) were then normalized to relative membrane expression for each mutant transporter.

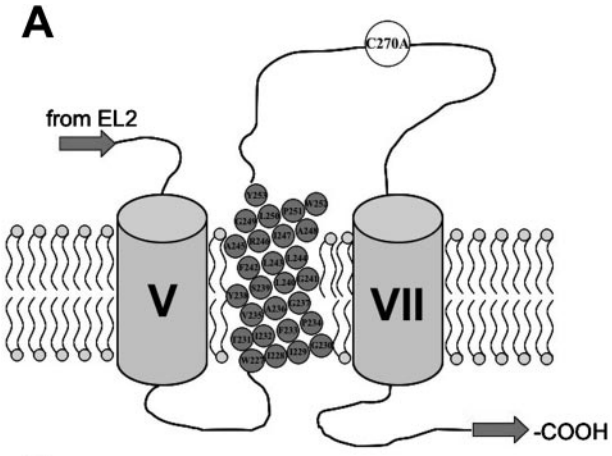

Fig. 1. Multiple sequence alignment of TM6 amino acids. A, secondary structure model of the last three transmembrane domains (TMDs) of hASBT according to the 7TM model. Roman numerals indicate flanking TMD, whereas TMD 6 amino acids are represented by gray circles inscribed with amino acid identity and position. Phospholipids of plasma membrane represented by circle (polar phosphate head group) with two tails (hydrophobic lipids). Top, exofacial; bottom, cytosolic. B, sequence alignment of amino acids 227 to 253, putatively forming TM6, for all known ASBT paralogs. Sequences were retrieved from GeneBank and aligned via the MULTALIN routine with annotation performed via the MPSA program. Shaded regions denote complete amino acid conservation among all species. Amino acid positioning relative to human ASBT is indicated by numbering on top. Bottom line indicates primary consensus for the TM6 region.

After data normalization (Fig. 2D), most TM6 mutants retained appreciable levels of activity, except for five mutants either severely hampered (I229C, G249C) or inactivated (P234C, G237C, G241C) upon cysteine substitution. Only P234C lacked expression in biotinylated (Fig. 2B) and whole-cell (data not shown) extracts. This may be due to disruptions in protein synthesis, but more likely, alterations in protein folding and stability occur that induce rapid protein degradation via endoplasmic reticulum-associated machinery. It is interesting that all five residues are conserved among known species of ASBT (Fig. 1B), suggesting primary roles in transport function that necessitate preservation of these amino acids. Because of their low activity levels, these mutants were excluded from further studies.

TM6 Mutants Demonstrated Substantial Na^+ Sensitivity. As a Na^+ cotransporter, ASBT activity relies on proper recognition, binding, and translocation of two Na^+ ions per one bile acid molecule (Weinman et al., 1998). Thus, we examined the consequences of equilibrative extracellular Na^+ concentrations upon mutant activity. For each mutant, the ratio of transport rates at equilibrative (12 mM) versus physiological (137 mM) Na^+ concentrations was calculated and expressed as a percentage of the C270A Na^+ ratio. This experimental scheme may uncover hidden functional defects in mutants otherwise unaffected by cysteine mutation. Therefore, the C270A parental construct displays a Na^+ ratio of 0.70 ± 0.04 (data not shown), indicating minimal consequences to transporter function upon alanine substitution at the native cysteine residue. In contrast, significant decreases in activity were observed for the majority (~64%) of TM6 cysteine mutants. Of 21 mutants assayed, 14 demonstrated hampered uptake rates at equilibrative [Na^+] (Fig. 3). EL3 cysteine mutants from our earlier study also exhibited similarly extensive Na^+ sensitivity (Banerjee et al., 2008), wherein uptake activities of 90% of assayed mutants were susceptible to equilibrative [Na^+]. Because EL3 residues putatively form Na^+ interaction sites (Banerjee et al., 2008), the widespread Na^+-dependence observed for TM6 mutants implies their close proximity to such Na^+ interaction sites and lends credence to TM6 participation during Na^+ permeation.

Substrate and Cation Binding Modulate Accessibility of Cysteine Mutants to MTS Modification. Both positively and negatively charged MTS reagents were used to probe the solvent accessibility of 21 cysteine mutants demonstrating measurable uptake activity. Intact monolayers of COS-1 cells expressing mutant transporters were preincubated with 1.0 mM concentration of either MTSES, MTSET, or MTSEA followed by uptake assessments. MTSET (109 $Å^3$) and MTSES (90 $Å^3$) exhibited similar inhibition profiles, in which activities of only mutants V235C, S239C, F242C, and R246C were significantly reduced (data not shown), suggesting minimal electrostatic effects in accessibility at those sites. The remainder of the TM6 mutants assayed were either inaccessible to these MTS reagents, or their modification was functionally silent. Incubation with the relatively smaller MTSEA (69 $Å^3$) inhibited uptake at sites accessed by the larger MTS reagents (i.e., V235C, S239C,

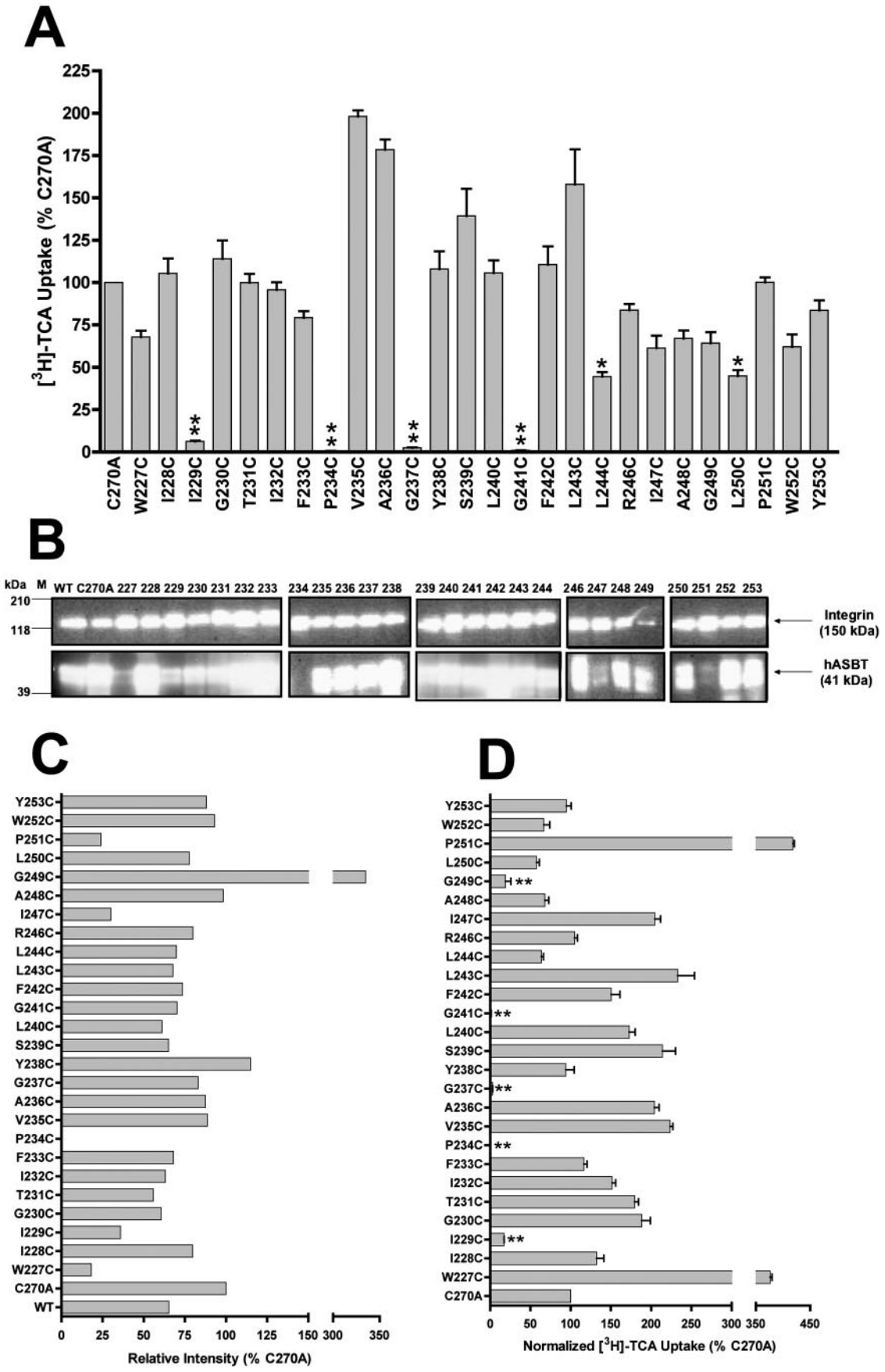

Fig. 2. [^{3}H]TCA uptake activity and membrane expression of TM6 cysteine mutants. A, uptake of [^{3}H]TCA was measured in COS-1 cells as described under *Materials and Methods* and expressed as a percentage of the parental transporter C270A. B, intact transfected COS-1 cells were treated with

F242C, and R246C; Fig. 4) and at two additional sites (A248C and Y253C; Fig. 4).

Because MTSEA (1 mM) application produced the most pronounced inhibition of the three MTS reagents used (similar to our previous study with TM7; Hussainzada et al., 2006), the effects of Na^+ and bile acid substrate on MTSEA accessibility of mutants V235C, S239C, F242C, R246C, A248C, and Y253C was evaluated. Our previous studies with EL3 and TM7 have shown that coincubation of MTS reagents with bile acids and/or removal of Na^+ from the preincubation buffer caused a reversal of the inhibitory effect observed with MTS incubation alone (Hussainzada et al., 2006; Banerjee et al., 2008). Likewise, in the present study, all TM6 mutants inhibited by MTSEA (1 mM) demonstrated significant uptake recovery when MTSEA incubation was performed in the absence of Na^+ and/or presence of 1.0 mM glycodeoxycholic acid (GDCA) (Fig. 4). In particular, the removal of Na^+ from the MTSEA preincubation medium significantly restored transport activity for mutants V235C, S239C, F242C, R246C, and A248C, whereas coincubation with GDCA (K_m = 2.0 ± 0.4 μM) significantly protected mutants F242C and A248C. Concurrent removal of Na^+ and the addition of the high-affinity substrate GDCA (1 mM) resulted in significant MTSEA protection for mutants V235C, S239C, F242C, and R246C. In all cases, mutant activities were restored to control (C270A) levels (within standard deviation; Fig. 4).

Although mechanistic details of the ASBT translocation cycle are as yet unresolved, ordered binding of ligands followed by translocation probably occurs, similar to many other Na^+-coupled transporters (Quick and Jung, 1997; Jung, 2001; Pajor and Randolph, 2005; Zhang and Rudnick, 2005). In this scenario, the ordered binding of Na^+ and bile acids would trigger the protein to assume various discrete structural conformations, eventually leading to carrier reorientation within membrane leaflets and substrate turnover. Within TM6, the lack of Na^+ binding events (simulated by substitution of Na^+ with $choline^+$ in preincubation buffers) significantly decreased MTSEA modification rates for all sites (Fig. 4), suggesting that protein conformational states assumed before the binding of Na^+ occlude these thiol groups from subsequent modification. Furthermore, the binding of bile acid substrate (GDCA) in either the presence or absence of Na^+ also triggers protein conformations that significantly decrease MTSEA access to all sites (Fig. 4). Because of the close association between TM6 and protein regions previously implicated during ligand binding and translocation (i.e., TM7 and EL3), the observed substrate protection may result from 1) occlusion of these sites via conformational changes; 2) the physical presence of substrates preventing access; or 3) a combination of both scenarios. The alternating accessibility of TM6 sites to thiol modification suggests the first scenario, whereas the restoration of mutant activity to control levels via substrate protection infers the second scenario. It is likely that a union of both situations prevails, in which TM6 residues may line portions of the permeation pore and also transduce conformational changes resulting from ligand interactions at adjacent protein regions (TM7, EL3), although further studies are needed to unequivocally conclude the origin of substrate protection. However, it is noteworthy that our data highlight a trend toward protection from MTS modification in the absence of Na^+, which is entirely plausible given that EL3 residues contain putative Na^+ interaction sites (Banerjee et al., 2008). It may be that the lack of Na^+ binding at EL3 regions prevents downstream conformational changes that "open" TM6 residues to MTS modification. Overall, we conclude that TM6 amino acids probably line portions of the substrate permeation route due to their spatial proximity with EL3 and TM7 residues and their solvent-accessibility profile.

Mutation of Pro234 Affects Both Transporter Expression and Function. Because the P234C double mutant (C270A/P234C) lacked expression both at the plasma membrane (Fig. 2B) and in whole-cell extracts (data not shown), additional replacements were made at this site to determine whether Pro234 makes functional contributions during the hASBT transport cycle. Using the wild-type (*WT*) species as the scaffold, alanine, glycine, and cysteine replacements were incorporated and analyzed with respect to uptake activity and membrane expression. As expected from our results using the kinetically similar C270A template (Banerjee et al., 2005), the P234C mutant constructed against the *WT* background lacked expression both in membrane (Fig. 5B) and whole-cell (Fig. 5C) extracts, confirming that cysteine replacement at this position affects transporter expression levels irrespective of the mutational template used. Glycine replacement (P234G) also seems to disrupt protein expression, resulting in minimal transporter expression in membrane (Fig. 5B) and whole-cell (Fig. 5C) extracts. In contrast, the alanine mutant (P234A) displayed plasma membrane expression, albeit at reduced levels (30% of C270A levels; Fig. 5A). After normalization to cell surface expression levels, uptake function of the P234A mutant remained severely inhibited (Fig. 5A), suggesting functional and structural impairments to transporter function. Defective trafficking to the plasma membrane may account for the lowered membrane expression of the P234A mutant, because the ratio of its plasma membrane expression to whole-cell expression is approximately half of the similar ratio for the *WT* species (i.e., 0.452 versus 0.814); however, further studies are needed for unequivocal evidence. We conclude that Pro234 participates in both protein expression and transporter function, confirming the overall importance of this atypical amino acid.

Discussion

This article details the solvent accessible sites along TM6 of hASBT as revealed by SCAM). This follows as a logical extension of our previous studies using this methodology that revealed putative Na^+ and substrate interaction sites along

sulfo-NHS-SS-biotin as described under *Materials and Methods* followed by Western blot processing. Blots were probed with the anti-hASBT antibody (1:30,000 dilution) followed by horseradish peroxide-linked anti-rabbit immunoglobin (1:2000 dilution). Each blot was probed for the internal plasma membrane marker α-integrin (150 kDa) and the absence of calnexin (90 kDa) (data not shown), an endoplasmic reticulum membrane protein representing the negative control in the biotinylated fractions. Marker lanes are shown on the left side of the individual blots. Mature glycosylated hASBT visualizes as the 41-kDa band, whereas the lower 38-kDa band (not shown) represents the unglycosylated species. C, densitometric analysis for cysteine mutants normalized to internal marker (α-integrin) and represented as a percentage of C270A parent. D, [^{3}H]TCA uptake activity normalized to relative cell surface expression. Bars represent mean ± S.D. of three separate experiments with ***, $p \leq 0.001$; **, $p \leq 0.01$; and *, $p \leq 0.05$, respectively, using analysis of variance with Dunnett's post hoc analysis.

EL3 (Banerjee et al., 2008) and demonstrated TM7 participation during substrate permeation (Hussainzada et al., 2006). Here, the key findings include: 1) identification of a TM6 helical face demonstrating significant MTS accessibility; 2) modulation of thiol modification rates along this helical face via Na^+ and bile acid binding events; 3) the spatially intimate association of MTS-accessible TM6 amino acids with functionally important TM7 residues; and, finally, 4) identification of a potential "conformational switch" necessary for substrate permeation that lines a helical face spatially distinct from the MTS-accessible face of TM6.

Of the 26 amino acids constituting TM6, the majority proved tolerant to cysteine substitution, whereas 5 were either functionally inactive (P234C, G237C, G241C) or significantly hampered (I229C, G249C) upon mutation (Fig. 2D). With the exception of Ile229, these residues en bloc display an approximate α-helical periodicity (Fig. 6B). It is interesting that cysteine substitution at Pro234 decreased protein expression levels, as evidenced by a lack of expression during immunoblotting of membrane (Fig. 2B) and whole-cell (data not shown) protein fractions. To determine whether Pro234 contributes in a functional capacity during ASBT transport, additional amino acid substitutions were incorporated using the native (WT) protein template (which kinetically behaves very similarly to the C270A construct required for thiol modification studies). Again, cysteine and glycine replacement severely decreased whole-cell protein expression levels (Fig. 5C), suggesting disruptions during either protein synthesis or, more likely, protein folding and stability that lead to rapid degradation. Only alanine substitution (P234A) at this site resulted in significant membrane expression; however transport function remained abrogated (Fig. 5). Thus, the highly conserved Pro234 functions in a dual capacity, probably essential for both proper protein expression and function. This two-pronged contribution of prolines, especially those situated in membrane segments, has been documented previously for many other important solute carriers and exchangers as well (Lin et al., 2000; Lu et al., 2001; Shelden et al., 2001; Labro et al., 2003; Slepkov et al., 2004; Joshi and Pajor, 2006). As observed by Kaback and colleagues for *Lac per-*

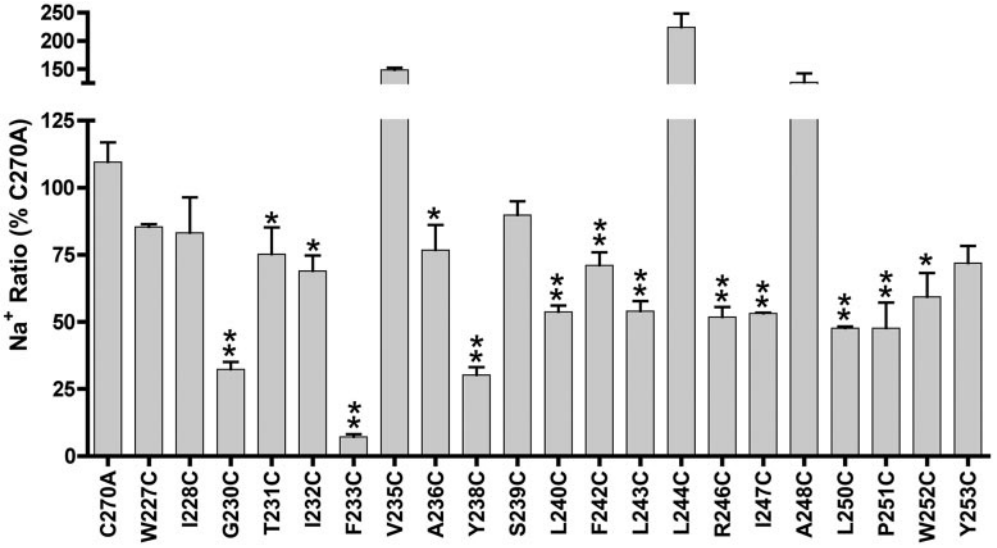

Fig. 3. Sodium sensitivity of cysteine mutants. COS-1 cells expressing mutant transporters were incubated in uptake medium (5 μM [^{3}H]TCA) containing low (12 mM) or physiological (137 mM) Na^+ concentrations as described under *Materials and Methods*. Sodium ratios were calculated for each mutant as the quotient of activity at 12 versus 137 mM [Na^+] and expressed as a percentage of C270A. Bars represent mean activity ± S.D. (n = 3). *, $p \leq 0.05$.

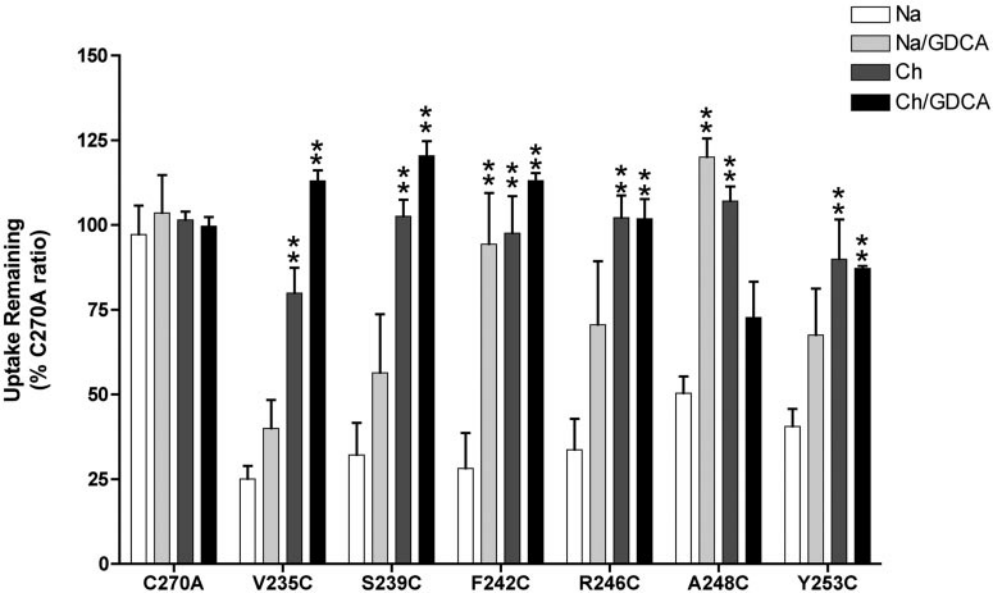

Fig. 4. Cation and substrate protection of TM6 cysteine mutants. Transiently transfected COS-1 cells expressing TM6 cysteine mutants were preincubated in buffer, pH 7.4, containing 1 mM MTSEA and either 137 mM NaCl (□), 137 mM NaCl and 1 mM GDCA (gray bar); 137 mM choline chloride (dark gray bar); or 137 mM choline chloride and 1 mM GDCA (■) and followed by [^{3}H]TCA uptake as described under *Materials and Methods*. Choline chloride does not activate the transporter and provides equimolar replacement for NaCl. All control wells were treated identically. Bars represent mean ± S.D. of at least three separate measurements. Data are expressed as a percentage of C270A values for each condition as described under *Materials and Methods*. Student's t test analysis performed with *, $p < 0.05$, and **, $p < 0.01$.

mease, a paradigm of secondary active transporters, relatively few amino acids are essential for transport unless directly involved in forming linkages with substrate; instead, such carriers must be "highly flexible proteins capable of widespread conformational changes during turnover" (Kaback and Wu, 1997). Because membrane-bound carriers are tightly woven through the lipid bilayer, usually via multiple transmembrane segments, such flexibility is not inherent and must instead be imparted by specific residues situated along the protein. Proline residues, specifically, can impart this flexibility, because they cyclize back onto their backbone nitrogen atom and prevent hydrogen bonding between protons of the ith residue to $(i-4)^{th}$ carbonyl oxygens, a requirement for maintaining classic α-helical structure (Woolfson and Williams, 1990) and ultimately destabilize the helix and increase overall flexibility (Bright et al., 2002; Cordes et al., 2002). Such perturbations of backbone dihedral angles of α-helices that lead to increased flexibility are also observed with glycine residues, albeit to a lesser extent (Javadpour et al., 1999; Cordes et al., 2002). It is compelling that a total of four glycine (Gly230, Gly237, Gly241, and Gly249) and two proline (Pro234 and Pro251) residues line the TM6 helix (Fig. 1B), of which all except for Pro251 are conserved among all known species of ASBT (Fig. 1B). Therefore, with the exception of Gly230 and Pro251, these residues were found to be essential for transport function of ASBT (Fig. 2). Thus, glycines, and particularly prolines, may impart the necessary flexibility required to assume discrete protein conformational states during substrate turnover. It is interesting that numerous studies (Gibbs et al., 1997; Javadpour et al., 1999; Tieleman et al., 1999) have noted the preferred pairing of proline and glycine residues, particularly at positions lining a shared helical face, which may reflect possible modulation of proline-induced distortions by the presence of similarly "flexible" glycine residues. We observe this trend for inactive mutants P234A, G237C, G241C, and G249C, which approximately line a single helical face (Fig. 6B) that could facilitate potential glycine modulation of Pro234-induced helical distortions. Finally, in the case of G230C and P251C, substantial loss of activity occurs in equilibrative Na^+ concentrations, suggesting auxiliary roles for these residues during the translocation cycle, possibly in transduction of conformational signals.

Superimposed on a secondary structural model of ASBT, our en masse MTS inhibition profiles generated thus far (Fig. 6A) strongly implicate the participation of TM6 residues during substrate translocation as well. Using physicochemically diverse thiol modifiers, four sites were significantly inhibited by preincubation with either 1.0 mM MTSES or MTSET (Val235, Ser239, Phe242, and Arg246; data not shown), whereas MTSEA application (1.0 mM) inhibited six sites total (Val235, Ser239, Phe242, Arg246, Ala248, and Tyr253; Fig. 4). Based on its similar MTS inhibition profiles, electrostatic and steric effects minimally influence TM6 modification rates. Using our in silico three-dimensional model (Zhang et al., 2004; Banerjee and Swaan, 2006), four MTS-

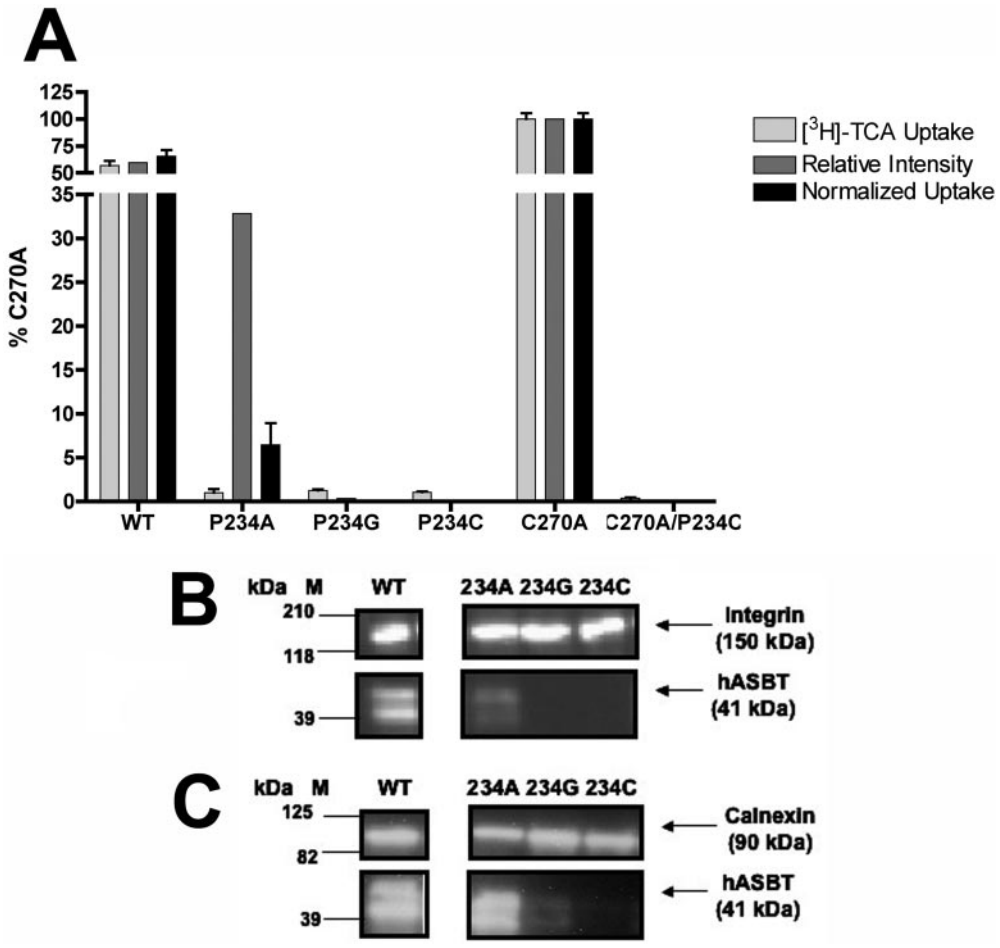

Fig. 5. [^{3}H]TCA uptake and membrane expression of Pro234 mutants. A, the initial [^{3}H]TCA uptake (gray bars), relative intensity of immunoblotting (dark gray bars), and normalized uptake activities (black bars) for Pro234 single and double mutants and their parental templates are depicted. Bars represent mean ± S.D. of at least three separate measurements. Data are expressed as a percentage of C270A values for each condition. Student's t test analysis was performed with *, $p < 0.05$, and **, $p < 0.01$. Activities of the Pro234 constructs are statistically different from both WT and C270A ($p < 0.01$); however, asterisks (**) have been omitted for visual clarity. B, intact transfected COS-1 cells were treated with sulfo-NHS-SS-biotin as described under *Materials and Methods* followed by Western blot processing. Marker lanes are shown on the left side of the individual blots. Mature glycosylated hASBT visualizes as the 41-kDa band, whereas the lower 38-kDa band (not shown) represents the unglycosylated species. C, immunoblotting of whole-cell extracts from transfected COS-1 cells as described under *Materials and Methods* showing glycosylated (41 kDa) and unglycosylated (38 kDa) hASBT species.

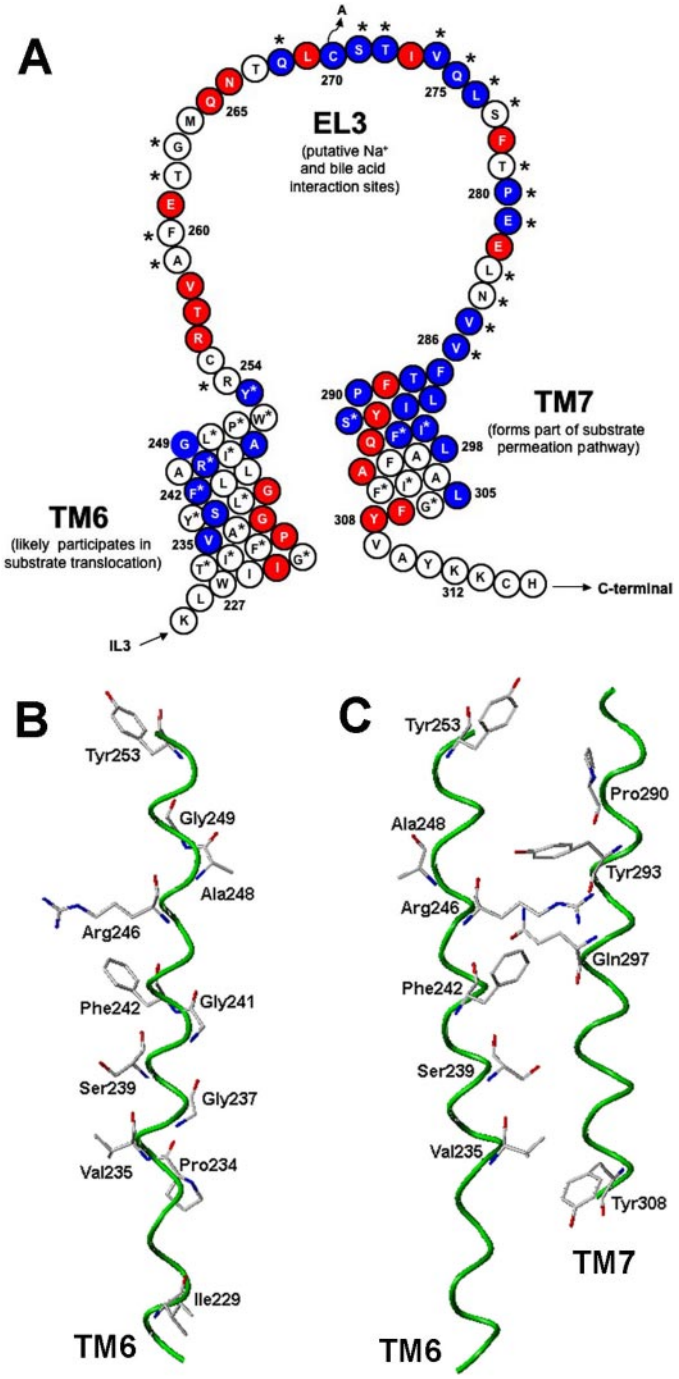

Fig. 6. ASBT MTS inhibition profile and TM6 in silico model. A, secondary structural model of hASBT regions submitted to SCAM analysis thus far. Red shading indicates residues inactivated by cysteine substitution, whereas blue shading indicates significant ($p < 0.05$) MTS inhibition. Asterisks (*) indicate significant ($p < 0.05$) Na^+ sensitivity. Taken en masse, our MTS inhibition data reflect the widespread solvent accessibility of these protein regions, corroborating their roles in ligand interaction and translocation. The prevalence of mutation-inactivated sites also confirms the essential nature of amino acids lining these protein segments. As noted, our earlier studies putatively assign ligand interaction sites along EL3 and TM7 with the substrate permeation path comprising TM7 (Hussainzada et al., 2006) and probably TM6 amino acids. B, in silico prediction of functional group orientation of TM6 sites inhibited by 1 mM MTSEA and protected by GDCA addition (1 mM) or Na^+ removal from MTS preincubation medium (i.e., Val235, Ser239, Phe242, Arg246, Ala248, and Tyr253). Also shown are the spatially distinct mutation-inactivated sites (Ile229, Pro234, Gly237, Gly241, and Gly249). Occurrence of proline and multiple glycine residues along inactivated helical face indicates functional requirement for helical flexibility crucial for transporter activity; C, in silico prediction of spatially intimate association of TM6 amino acids demonstrating MTSEA inhibition and substrate protection (i.e., Val235, Ser239, Phe242, Arg246, and Tyr253) and TM7 residues shown previously as either highly MTS-accessible (Pro290 and Ser294) or inactivated by cysteine substitution (Tyr293, Gln297, and Tyr308) (Hussainzada et al., 2006). In silico model spans amino acids Trp227 to Tyr253 (TM6) and Phe286 to Tyr308 (TM7) and was generated using THREADER with visualization by SYBYL 6.9 (3). Top, exofacial; bottom, cytosolic.

modified sites (Val235, Ser239, Phe242, and Arg246) exhibiting an α-helical periodicity were found to line a TM6 face spatially distinct from the proline and glycine "conformational switch" discussed above (Fig. 6B). Next, we modeled the functional group orientation of these four TM6 residues with respect to TM7 residues implicated previously in lining the substrate permeation path (Hussainzada et al., 2006) to determine the spatial feasibility of TM6 participation during translocation (Fig. 6C). It is striking that the functional groups of the four MTS-accessible TM6 sites (Val235, Ser239, Phe242, and Arg246) are situated in line with TM7 sites shown previously to be either highly MTS-accessible (Pro290, Ser294) or inactivated by mutation (Tyr293, Gln297, and Tyr308). Thus, our in silico model may delineate the shared solvent-accessible molecular spaces between TM7 and TM6 residues. It is tempting to speculate that such communal volumes of molecular space could form a translocation route to enable transfer of charged substrates across the forbiddingly hydrophobic environment of the lipid bilayer. The presence of polar (Ser239, Ser294, and Gln297) and charged (Arg246) residues along the collective TM7–TM6 "pathway" strengthens this hypothesis, because they may form hydrophilic surfaces promoting Na^+ and bile acid movement into the cell interior (Fig. 6C). Further validation of the in silico hypotheses can be inferred from our experimental data, in particular substrate protection studies of the six MTSEA-accessible TM6 mutants. Removal of Na^+ or addition of the high-affinity substrate GDCA (1.0 mM) to the MTSEA (1.0 mM) preincubation medium significantly decreased MTSEA modification rates for all inhibited sites, such that mutant activities were restored to C270A control levels (Fig. 4). Thus, our experimental results suggest the physical presence of substrates in or around these sites predicted previously in silico as forming translocation paths with TM7. Integrating our in silico model, MTS inhibition profiles, and mutagenesis results, we can speculate that the TM6 "conformational switch" (i.e., Pro234, Gly237, Gly241, and Gly249C) functions to promote helical flexibility necessary for widespread protein conformational changes triggered after ligand binding, whereas the spatially distinct solvent-accessible face (i.e., Val235, Ser239, Pro242, and Arg246) forms putative permeation routes with TM7 (and probably other protein regions) during substrate turnover. Loss of TM6 helical flexibility, as occurs upon replacement of the highly helix-distorting Pro234 with the more rigid alanine (P234A), renders the transporter incapable of the changes in protein structure that are a necessary prerequisite for function.

Finally, the ubiquitous Na^+ sensitivity of TM6 residues is unsurprising, because it suggests proximity of this protein region to putative Na^+ interaction sites. Because EL3 residues link TM6 and TM7 helical segments and our earlier study demonstrates Na^+ interaction sites along EL3 (Baner-

jee et al., 2008), amino acid mutation along TM6 probably perturbs efficient transduction of conformational changes triggered after Na^+ binding along EL3 contact points. Although these consequences are masked at physiological [Na^+], equilibrative Na^+ concentrations expose the functional defects resulting from mutagenesis of this protein region. Of 22 mutants assayed, ~64% exhibited significant decreases in activity at equilibrative Na^+ concentrations; furthermore, of those mutants affected, approximately 71% demonstrated less than half of their original activity (Fig. 3). As mentioned earlier, G230C and P251C are included in this category, reinforcing the contribution of helical flexibility to ASBT function. Overall, the widespread and severe response of TM6 cysteine mutants to reduced levels of extracellular Na^+ infers the proximity of this region to Na^+ binding sites while supporting a functional role for TM6 amino acids during ASBT transport.

In conclusion, analysis of data generated via cysteine-scanning mutagenesis of TM6 in the context of our previous SCAM studies and homology model has provided novel insight into the molecular workings of the ASBT translocation cycle. In accord with our earlier work, putative ligand binding domains and portions of the substrate permeation pathway were identified (Hussainzada et al., 2006; Banerjee et al., 2008); in the present manuscript, we demonstrate a functional prerequisite for TM6 helical flexibility in global conformational changes to protein structure leading to substrate turnover and the putative involvement of TM6 amino acids in lining portions of the permeation pathway.

References

Balakrishnan A and Polli JE (2006) Apical sodium dependent bile acid transporter (ASBT, SLC10A2): a potential prodrug target. *Mol Pharm* **3:**223–230.

Banerjee A, Hussainzada N, Khandelwal A, and Swaan PW (2008) Electrostatic and potential cation-pi forces guide interaction of extracellular loop III in human apical sodium-dependent bile acid transporter (hASBT) with Na^+ and bile acids. *Biochem J,* in press.

Banerjee A, Ray A, Chang C, and Swaan PW (2005) Site-directed mutagenesis and use of bile acid-MTS conjugates to probe the role of cysteines in the human apical sodium-dependent bile acid transporter (SLC10A2). *Biochemistry* **44:**8908–8917.

Banerjee A and Swaan PW (2006) Membrane topology of human ASBT (SLC10A2) determined by dual label epitope insertion scanning mutagenesis. New evidence for seven transmembrane domains. *Biochemistry* **45:**943–953.

Bright JN, Shrivastava IH, Cordes FS, and Sansom MS (2002) Conformational dynamics of helix S6 from Shaker potassium channel: simulation studies. *Biopolymers* **64:**303–313.

Chiang JY, Kimmel R, and Stroup D (2001) Regulation of cholesterol 7alpha-hydroxylase gene (CYP7A1) transcription by the liver orphan receptor (LXRalpha). *Gene* **262:**257–265.

Cordes FS, Bright JN, and Sansom MS (2002) Proline-induced distortions of transmembrane helices. *J Mol Biol* **323:**951–960.

Deber CM, Glibowicka M, and Woolley GA (1990) Conformations of proline residues in membrane environments. *Biopolymers* **29:**149–157.

Geyer J, Wilke T, and Petzinger E (2006) The solute carrier family SLC10: more than a family of bile acid transporters regarding function and phylogenetic relationships. *Naunyn Schmiedebergs Arch Pharmacol* **372:**413–431.

Gibbs N, Sessions RB, Williams PB, and Dempsey CE (1997) Helix bending in alamethicin: molecular dynamics simulations and amide hydrogen exchange in methanol. *Biophys J* **72:**2490–2495.

Hallén S, Bjorquist A, Ostlund-Lindqvist AM, and Sachs G (2002) Identification of a region of the ileal-type sodium/bile acid cotransporter interacting with a competitive bile acid transport inhibitor. *Biochemistry* **41:**14916–14924.

Hallén S, Fryklund J, and Sachs G (2000) Inhibition of the human sodium/bile acid cotransporters by side specific methanethiosulfonate sulphydryl reagents: substrate controlled accessibility of site of activation. *Biochemistry* **39:**6743–6750.

Huff MW, Telford DE, Edwards JY, Burnett JR, Barrett PH, Rapp SR, Napawan N, and Keller BT (2002) Inhibition of the apical sodium-dependent bile acid transporter reduces LDL cholesterol and apoB by enhanced plasma clearance of LDL apoB. *Arterioscler Thromb Vasc Biol* **22:**1884–1891.

Hussainzada N, Banerjee A, and Swaan PW (2006) Transmembrane domain VII of the human apical sodium-dependent bile acid transporter ASBT (SLC10A2) lines the substrate translocation pathway. *Mol Pharmacol* **70:**1565–1574.

Izzat NN, Deshazer ME, and Loose-Mitchell DS (2000) New molecular targets for cholesterol-lowering therapy. *J Pharmacol Exp Ther* **293:**315–320.

Javadpour MM, Eilers M, Groesbeek M, and Smith SO (1999) Helix packing in polytopic membrane proteins: role of glycine in transmembrane helix association. *Biophys J* **77:**1609–1618.

Joshi AD and Pajor AM (2006) Role of conserved prolines in the structure and function of the Na^+/dicarboxylate cotransporter 1, NaDC1. *Biochemistry* **45:**4231–4239.

Jung H (2001) Towards the molecular mechanism of Na^+/solute symport in prokaryotes. *Biochim Biophys Acta* **1505:**131–143.

Kaback HR and Wu J (1997) From membrane to molecule to the third amino acid from the left with a membrane transport protein. *Q Rev Biophys* **30:**333–364.

Kramer W, Girbig F, Glombik H, Corsiero D, Stengelin S, and Weyland C (2001) Identification of a ligand-binding site in the Na^+/bile acid cotransporting protein from rabbit ileum. *J Biol Chem* **276:**36020–36027.

Labro AJ, Raes AL, Bellens I, Ottschytsch N, and Snyders DJ (2003) Gating of shaker-type channels requires the flexibility of S6 caused by prolines. *J Biol Chem* **278:**50724–50731.

Li H, Xu G, Shang Q, Pan L, Shefer S, Batta AK, Bollineni J, Tint GS, Keller BT, and Salen G (2004) Inhibition of ileal bile acid transport lowers plasma cholesterol levels by inactivating hepatic farnesoid X receptor and stimulating cholesterol 7 alpha-hydroxylase. *Metabolism* **53:**927–932.

Lin Z, Itokawa M, and Uhl GR (2000) Dopamine transporter proline mutations influence dopamine uptake, cocaine analog recognition, and expression. *FASEB J* **14:**715–728.

Lu H, Marti T, and Booth PJ (2001) Proline residues in transmembrane alpha helices affect the folding of bacteriorhodopsin. *J Mol Biol* **308:**437–446.

Mitchell SM, Lee E, Garcia ML, and Stephan MM (2004) Structure and function of extracellular loop 4 of the serotonin transporter as revealed by cysteine-scanning mutagenesis. *J Biol Chem* **279:**24089–24099.

Oelkers P, Kirby LC, Heubi JE, and Dawson PA (1997) Primary bile acid malabsorption caused by mutations in the ileal sodium-dependent bile acid transporter gene (SLC10A2). *J Clin Invest* **99:**1880–1887.

Pajor AM and Randolph KM (2005) Conformationally sensitive residues in extracellular loop 5 of the Na^+/dicarboxylate co-transporter. *J Biol Chem* **280:**18728–18735.

Pauli-Magnus C, Stieger B, Meier Y, Kullak-Ublick GA, and Meier PJ (2005) Enterohepatic transport of bile salts and genetics of cholestasis. *J Hepatol* **43:**342–357.

Quick M and Jung H (1997) Aspartate 55 in the Na^+/proline permease of Escherichia coli is essential for Na^+-coupled proline uptake. *Biochemistry* **36:**4631–4636.

Sansom MS and Weinstein H (2000) Hinges, swivels and switches: the role of prolines in signalling via transmembrane alpha-helices. *Trends Pharmacol Sci* **21:**445–451.

Shelden MC, Loughlin P, Tierney ML, and Howitt SM (2001) Proline residues in two tightly coupled helices of the sulphate transporter, SHST1, are important for sulphate transport. *Biochem J* **356:**589–594.

Slepkov ER, Chow S, Lemieux MJ, and Fliegel L (2004) Proline residues in transmembrane segment IV are critical for activity, expression and targeting of the Na^+/H^+ exchanger isoform 1. *Biochem J* **379:**31–38.

Swaan PW, Hillgren KM, Szoka FC Jr, and Oie S (1997) Enhanced transepithelial transport of peptides by conjugation to cholic acid. *Bioconjug Chem* **8:**520–525.

Tieleman DP, Sansom MS, and Berendsen HJ (1999) Alamethicin helices in a bilayer and in solution: molecular dynamics simulations. *Biophys J* **76:**40–49.

Trauner M and Boyer JL (2003) Bile salt transporters: molecular characterization, function, and regulation. *Physiol Rev* **83:**633–671.

Weinman SA, Carruth MW, and Dawson PA (1998) Bile acid uptake via the human apical sodium-bile acid cotransporter is electrogenic. *J Biol Chem* **273:**34691–34695.

Wong MH, Oelkers P, and Dawson PA (1995) Identification of a mutation in the ileal sodium-dependent bile acid transporter gene that abolishes transport activity. *J Biol Chem* **270:**27228–27234.

Woolfson DN and Williams DH (1990) The influence of proline residues on alpha-helical structure. *FEBS Lett* **277:**185–188.

Zhang EY, Phelps MA, Banerjee A, Khantwal CM, Chang C, Helsper F, and Swaan PW (2004) Topology scanning and putative three-dimensional structure of the extracellular binding domains of the apical sodium-dependent bile acid transporter (SLC10A2). *Biochemistry* **43:**11380–11392.

Zhang YW and Rudnick G (2005) Cysteine-scanning mutagenesis of serotonin transporter intracellular loop 2 suggests an α-helical conformation. *J Biol Chem* **280:**30807–30813.

Address correspondence to: Dr. Peter W. Swaan, Department of Pharmaceutical Sciences, University of Maryland, 621 HSF-II, 20 Penn Street, Baltimore, MD 21201. E-mail: pswaan@rx.umaryland.edu